Edge-Localized Modes Explained as the Amplification of Scrape-Off-Layer Current Coupling

L. J. Zheng,[1] H. Takahashi,[2] and E. D. Fredrickson[2]

[1]*Institute for Fusion Studies, University of Texas at Austin, Austin, Texas 78712, USA*

[2]*Princeton Plasma Physics Laboratory, Princeton University, Princeton, New Jersey 08543, USA*

(Received 27 September 2007; published 19 March 2008)

It is shown that the edge-localized modes (ELMs) observed in tokamak *H* mode discharges can be explained as external magnetohydrodynamic (MHD) mode amplification due to coupling with scrape-off-layer current. The proposed model offers a new ELM mechanism that produces a sharp onset and initial fast growth of magnetic perturbations even when the underlying equilibrium is only marginally unstable for a MHD mode and also a quick quenching after the bursting peak. The theory also reproduces various other ELM features.

DOI: 10.1103/PhysRevLett.100.115001 PACS numbers: 52.35.Py, 52.55.Fa, 52.55.Hc

Understanding the edge-localized modes (ELMs) in the *H* mode phase is important for tokamak confinement [1,2]. Various theories have been proposed to explain ELM excitation, such as peeling-ballooning modes [3], nonlinear ballooning modes [4], edge Taylor relaxation [5], and blob formation theories [6]. Bursts in the scrape-off-layer (SOL) current have been observed concurrently with ELMs ([7–9] and references therein). The possible connection between ELMs and SOL current bursting was pointed out in Ref. [7]. It is therefore of interest to clarify how the coupling of the SOL current to magnetohydrodynamic (MHD) modes could lead to ELM bursting.

In this Letter, we show that there is a positive feedback process between the external plasma modes and the SOL current (referred to as resistive SOL modes): The initial magnetic perturbation at the pedestal causes radial transport, that discharges the pedestal heat and particles to the SOL and results in the bursting of the SOL current. In turn, the SOL current bursting can induce a stronger magnetic perturbation at the pedestal. This positive feedback causes the resistive SOL modes to grow nonlinearly and sharply even near the linear MHD marginal stability limit, leading to the ELM burst.

Since most ELMs have high-n features, we focus our investigation on the high-n modes. Here, n is the toroidal mode number. Note that high-n modes usually decay rapidly before reaching the conducting wall, we can ignore the conducting wall effect and consequently assume that the vacuum region inside the vacuum chamber extends to ''infinity.'' The coordinate system (ψ, θ, ϕ) is employed, where ψ represents the poloidal magnetic flux, θ is the poloidal angle, and ϕ is the axisymmetric toroidal angle. The equilibrium magnetic field is expressed as $\mathbf{B} = \nabla\phi \times \nabla\psi + g(\psi)\nabla\phi$, where boldface indicates a vector quantity. We introduce ψ_{b-} and ψ_{b+} to designate, respectively, the radial locations for the interface between the plasma and the SOL current layer and the interface between the SOL current layer and the vacuum region outside the SOL current layer.

The equation describing the coupling of the MHD modes and the SOL current can be derived from Ampere's law with the generalized Ohm's law included

$$\nabla \times \delta\mathbf{B} = \mu_0 \delta\mathbf{J} = \mu_0\sigma\left(\mathbf{E} + \frac{\lambda}{e}\nabla T_e + \frac{1}{n_e e}\nabla P_e\right) - \mu_0 \mathbf{J}_0, \quad (1)$$

where $\delta\mathbf{B}$ and $\delta\mathbf{J}$ represent the perturbed magnetic field and the current density, μ_0 is the vacuum permeability, e is the charge, n, T, and P represent the density, temperature, and pressure, $\mathbf{E}$ is the electric field, the subscripts i and e denote the ion and electron species, the average conductivity is $\sigma = e^2\lambda_{11}L/(m_e\langle 1/n_e\tau_{ei}\rangle)$, τ_{ei} is the electron-ion collision time, the quantity $\lambda = \lambda_{12}/\lambda_{11} = 0.71$ applies for a deuterium plasma, where $\lambda_{11} = 1.975$ and $\lambda_{12} = 1.389$ are the Spizer-Harm coefficients [10], L specifies the field line length between two divertors, $m_{e,i}$ is the mass, and $\langle\cdots\rangle$ represents a field line average. Both conductive and thermal currents are included in Eq. (1). Since the current perturbation $\delta\mathbf{J}$ has to be evaluated nonlinearly, we have used the difference of the total current $\mathbf{J}$ (the first term on the right-hand side) and the initial current $\mathbf{J}_0$ before MHD activities appear, to calculate it in Eq. (1).

For simplicity, we consider the large aspect ratio limit and the single mode case. Applying the operator $\nabla r \cdot \nabla\times$ to Eq. (1), we obtain

$$\tau_w \frac{\partial \delta B_r}{\partial t} - b\frac{d\delta B_r}{dr}\bigg|_{\psi_{b-}}^{\psi_{b+}} = i\mu_0 w k_\theta \delta J_\parallel, \quad (2)$$

where r is the minor radius, k_θ represents the normalized wave number in θ coordinate, $\tau_w = \mu_0 w b \sigma$, b is the location in minor radius of the thin SOL current layer, and the subscript $\parallel$ denotes the projection parallel to the magnetic field lines. Note that the SOL width w is small (about 0.02 m). The radial magnetic field δB_r is assumed to be continuous across the SOL, as in the usual tearing mode treatment. We have noted that the edge plasma transport is different from the core plasma transport. Edge transport is nonaxisymmetric and exhibits ''intermittency'' [11]. The nonaxisymmetric nature of the SOL current during the ELM activities has been observed experimentally ([8] and references therein).

The SOL current in Eq. (2) can be expressed using the theory developed in Ref. [12]. Note that electrons and ions have vastly different mobilities in the SOL. We extend the SOL current expression in Ref. [12] to a two-fluid description for temperature. The SOL current can be therefore expressed as $J_{\|} = J_{\rm sat}\hat{J}_{\|}$, where

$$\hat{J}_{\|} = -\gamma_0\Big\{\frac{eV_0}{kT_{eh}} + (\ln 2 + 0.71)\Big(\frac{T_{ec}}{T_{eh}} - 1\Big) + \frac{T_{ec}}{T_{eh}}\ln\alpha_c - \ln\alpha_h + \ln\Big[\frac{1+\hat{J}_{\|}}{(1-\frac{j_{\rm sat,h}}{j_{\rm sat,c}}\hat{J}_{\|})^{T_{ec}/T_{eh}}}\Big] + \frac{1}{kT_{eh}}\int_h^c \frac{1}{n}\frac{dp_{ec}}{ds}ds\Big\},$$

$J_{\rm sat} = en[k(T_i + T_e)/m_i]^{1/2}$, k is the Boltzmann constant, V_0 represents the applied voltage between the hot and cold divertors, $\alpha = [m_i T_e/2\pi m_e(T_e + T_i)]^{1/2}$, the subscripts h and c denote the sheaths, respectively, at the hot and cold divertors, $\gamma_0 = \sigma kT_{eh}/(eLJ_{\rm sat})$, and s represents the field line arc length.

The jump of the radial derivative of the perturbed magnetic field on the left-hand side of Eq. (2) can be obtained by matching to the outside solutions as in the conventional tearing mode theory, yielding

$$\tau_w\frac{\partial\delta B_r}{\partial t} - \Delta'\delta B_r = i\mu_0 w k_\theta \delta J_{\|}, \tag{3}$$

where $\Delta' = bd\ln\delta B_r/dr|_{\psi_{b-}}^{\psi_{b+}}$ is the usual tearing mode parameter. In order to connect the peeling-ballooning theory, we introduce also the energy integral type of notation for Δ'. Since the experimental observation of the magnetic perturbations is at the conductor wall, one can mathematically model a distributed SOL current of finite but small thickness with a thin current sheet using the Green function method, just as the so-called "control surface" concept in Ref. [13]. In this description, the tearing mode parameter can be expressed as $\Delta' = -\{2m/[1 - (a/b)^{2m}]\}(\delta W_\infty/\delta W_b)$ [14]. Here, δW_∞ and δW_b represent the "no-wall" and "ideal wall" energy integrals, a is the minor radius of the plasma torus, and m is the poloidal mode number. Note that here the "wall" just represents the modeled thin current sheet. When a finite thickness layer is theoretically shrunk into a modeled current sheet, it yields space on both sides. This causes a modeled thin vacuum between the modeled thin SOL sheet and the core plasma in this description. Comparing our governing equation, Eq. (2), with the governing equation in the previous study of the SOL current effect in Ref. [15], one can see that the term on the right-hand side of Eq. (2) is new. The presence of this new term takes account of the fact that the radial transport from the pedestal plasma can change the SOL thermal properties and consequently the current it carries. It is due to this new term that Eq. (2) contains a positive feedback process between the resistive SOL modes δB_r and the SOL current $\delta J_{\|}$, which provides a physical explanation for ELMs observed experimentally.

To show this positive feedback process, we derive the analytical solution of Eq. (2),

$$\delta B_r = e^{\int^t \Delta' dt/\tau_w}\Big[i\mu_0 w k_\theta \int^t \delta J_{\|} e^{-\int^t \Delta' dt/\tau_w} dt/\tau_w + \delta B_{r0}\Big], \tag{4}$$

where δB_{r0} is a constant. The solution in Eq. (4) contains two parts: the solo resistive SOL mode solution (the second term) and the $\delta J_{\|}$ driven part (the first term in the square brackets on the right-hand side). In the case without the SOL current effect (i.e., $\delta J_{\|} = 0$), system is unstable, if $\mathrm{Re}\{\Delta'\} > 0$. Note that instabilities would reduce Δ' toward the stable direction in the usual quasilinear picture due to the induced radial transport. The magnetic perturbation δB_r does not explode without the SOL current coupling. Instead, with the SOL current taken into account, the first term on the right-hand side of Eq. (4) leads to a self amplification loop as follows: High-n resistive SOL modes δB_r can be excited above a critical plasma beta limit $\Delta' > 0$. The initial activities of the resistive SOL modes cause a radial transport, that discharges the pedestal heat and particles to the SOL and results in the initial bursting of the SOL current. In turn, the SOL current bursting on the right-hand side of Eq. (4) amplifies the magnetic perturbation δB_r and induces a stronger radial transport. Consequently, an even larger SOL current $\delta J_{\|}$ results. This positive feedback process explains the bursting nature of ELMs and SOL current. The radial transport also reduces the pedestal pressure gradient and leads the ELMs to damp away as the self amplification mechanism disappears. The positive feedback nature also leads ELMs to quench sharply. The ELM cycle repeats when heating again increases the beta value. This is a unique nonlinear amplification regime that occurs at the plasma edge. First, as observed experimentally [2], the influx of the electrons with pedestal temperature can cause a sudden rise in density in the divertor sheaths, due to the dislodgement of neutrals from the saturated target divertors. A sudden increase in sheath density can cause a rapid increase of the saturated current. Second, although $e^{\int^t \Delta' dt/\tau_w}$ tends to play a stabilizing role because the radial transport reduces the pedestal beta so that $\mathrm{Re}\{\Delta'\} < 0$, in the first term on the right-hand side of Eq. (4) $e^{-\int^t \Delta' dt/\tau_w}$ becomes an exponential amplification factor for the SOL current effect in this case. Note that, even if $\delta J_{\|} = \text{const}$, Eq. (4) still yields the mode growth of the type that is linear in time.

The positive feedback process examined above can be displayed numerically. A complete numerical simulation would require a global code which couples the nonlinear MHD, transport, SOL current, divertor sheath physics, and, etc. Since we focus only on revealing the amplification phenomenon, not on the details of the process, we instead use a simplified model to explain the physics.

We describe the pedestal temperature and density as follows:

$$T^p(t) = T^{p0}[1 + Q^h t - Q^{\mathrm{Tr}}(t)], \tag{5}$$

$$n^p(t) = n^{p0}[1 + D^h t - D^{\mathrm{Tr}}(t)], \tag{6}$$

where the temperature and density losses due to the radial transport are described as follows

$$Q^{\mathrm{Tr}}(t) = Q_0^{\mathrm{Tr}} \int_{t_c}^{t} \frac{dt}{\Delta t} \left| \frac{\delta B_r}{\Delta B} \right|^{\alpha_q} \left(\frac{T^p n^p}{T^{p0} n^{p0}} \right)^{\alpha_{\mathrm{pt}}},$$

$$D^{\mathrm{Tr}}(t) = D_0^{\mathrm{Tr}} \int_{t_c}^{t} \frac{dt}{\Delta t} \left| \frac{\delta B_r}{\Delta B} \right|^{\alpha_d} \left(\frac{T^p n^p}{T^{p0} n^{p0}} \right)^{\alpha_{\mathrm{pn}}}.$$

Here, T^{p0} and n^{p0} are the initial pedestal temperature and density, the constants Q^h and D^h describe the temperature and density rates of rise due to heating, t_c is the critical time when the linear resistive SOL modes become unstable, Q_0^{Tr} and D_0^{Tr} are constants specifying the strength of the radial transport, various constants $\alpha\ldots$ are introduced to describe the dependences of radial transport on the magnetic field and pressure, Δt is the normalization constant and is selected as the ELM pulse duration, and ΔB is the normalization factor for δB_r, specified by the typical experimentally observed value. For simplicity, the ion and electron species in the pedestal are assumed to have the same temperature and density.

The radial transport results in the increments of the SOL temperature and density. We describe the temperature for electron and ion species and density for both species at the divertor sheaths for $t \geq t_c + \delta t_e$ as follows:

$$T_{e,i}^d(t) = T_{e,i}^{d0}\Bigg[1 + R_{e,i}^t Q^{\mathrm{Tr}}(t - \delta t_{e,i}) - C_{e,i}^t \int_0^t \frac{dt}{\Delta t} \times \left(\frac{T_{e,i}^d}{T_{e,i}^{d0}} \right)^{\kappa_{e,i}^t} H(T_{e,i}^d - T_{e,i}^{d0}) \Bigg], \tag{7}$$

$$n^d(t) = S_n n^{d0}\Bigg[1 + R^n D^{\mathrm{Tr}}(t - \delta t_e) - C^n \int_0^t \frac{dt}{\Delta t} \times \left(\frac{n^d}{n^{d0}} \right)^{\kappa^n} H(n^d - n^{d0}) \Bigg], \tag{8}$$

where $T_{e,i}^{d0}$ and n^{d0} are the initial divertor sheath temperature and density, the constants $R_{e,i}^t$ and R^n describe, respectively, the coupling factors of the radial temperature and density transport, the constants $C_{e,i}^t$ and C^d describe the temperature and density cooling rates, and the Heaviside function $H(x) = 1$ for $x > 0$, otherwise 0. Note that, strictly speaking, $H(x) = 0$ does not represent that the cooling term is inactive, but the cooling (sink) and background transport from the core plasma (source) balance after ELM quench. In this way, we model the flat time evolution of the SOL density and temperature between two subsequent ELM burstings, as observed experimentally. We have introduced $S_n(t; \delta t_{e,i}) = S_n^0(\delta t_{e,i}) \times \{2 - \exp[-\lambda_s(t - t_c - \delta t_e)]\}$ to simulate the density increment due to the dislodgement of neutrals from the saturated divertor plates, where λ_s is a constant and $S_n^0(\delta t_{e,i})$ specifies the density amplification factor. Note that the perpendicular transport in the SOL can play a significant role for particle flux with long transit time δt. The perpendicular transport can smooth SOL temperature and density. Consequently, the nonaxisymmetric component coupled to the MHD modes in Eq. (4) becomes weaker. Therefore, one can expect $S_n^0(\delta t_{e,i})$ to be a decreasing function of $\delta t_{e,i}$. The ratio of the temperatures in the hot and cold divertor sheaths is employed as parameter. For simplicity, we have not taken into account the so-called divertor temperature instability [16]. We have also neglected other thermalization times for simplicity.

We describe the various energy integrals as follows: $\mathrm{Re}\{\delta W_\infty\} = C_w(-\beta + \beta_c)$ and $\delta W_b = \delta W_\infty + \delta W_v$, where C_w is a constant, $\beta = 2\mu_0 n^p T^p / B^2$ is the ratio of plasma to magnetic field pressures, β_c denotes the critical beta for no-wall stability, and δW_v represents the vacuum energy integral. In our numerical simulation δW_v and $\mathrm{Im}\{\delta W_{\infty,b}\}$ are employed as parameters. The set of equations, Eqs. (3) and (5)–(8), is solved as an initial value problem, with the parallel current and other thermal quantities, such as σ, updated at each time step. A typical numerical result is plotted in Fig. 1, with parameters given as follows: $a = 0.54$ m, $b = 1.02a$, $w = 0.02$ m, $m = 30$,

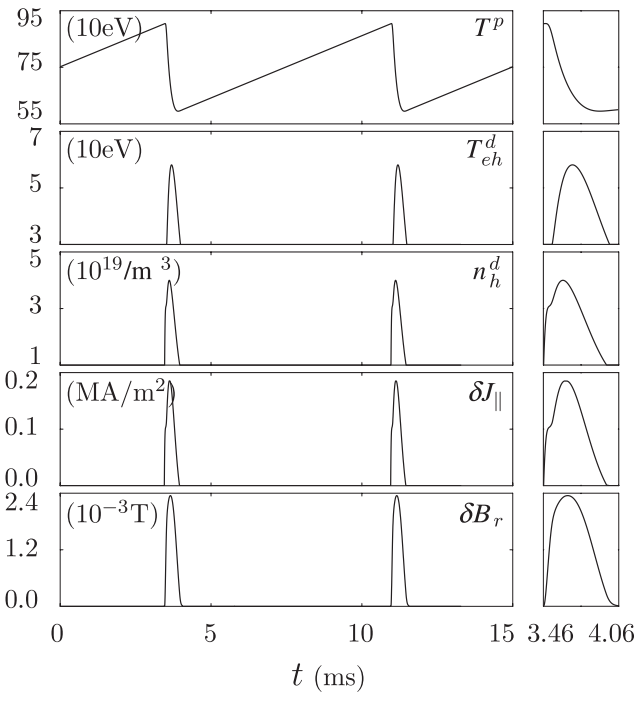

FIG. 1. Numerical results for ELMs. The first row describes the pedestal temperature evolution with time, the second and third give, respectively, the ion temperature and the ion or electron density in the hot divertor sheath, the forth is the SOL current, and the last gives the radial magnetic field δB_r. The right column is the high-time-resolution redisplay of the first ELM pulse in the left column.

$L = 100$ m, $\Delta t = 600$ μs, $\Delta B/\Delta t = 5$ T/s, $T^{p0} = 590$ eV, $n^{p0} = 9.7 \times 10^{19}$ 1/m^3, $Q^h = D^h = 201$, $Q_0^{\mathrm{Tr}} = D_0^{\mathrm{Tr}} = 0.41$, $\alpha_{\ldots} = 2$, $\delta W_v = 0.005$, $\mathrm{Im}\{\delta W_{\infty,b}\} = 0$, $\beta_c = 0.05$, $C_w = 1$, $T_{e,i}^{d0} = 30$ eV, $n^{d0} = 1 \times 10^{19}$ 1/m^3, $R_e^t = 5$, $R_i^t = 2$, $R^n = 3$, $C_e^t = 2.1$, $C_i^t = 1.4$, $C^n = 1.08$, $\delta B_{r0} = 10^{-5}$ T, $\kappa_{\vdots} = 1$, $T_h/T_c = 3$, $S_n^0 = 2$, $\lambda_s = 0.5/\delta t_e$, $\delta t_e = 10$ μs, and $\delta t_i = 100$ μs. For simplicity, we assume that $V_0 = dp_{ec}/ds = 0$. In Fig. 1, the ELM bursting and quenching are reproduced as the consequence of changing pedestal beta and varying SOL current. The δB_r growth exhibits two phases. As plasma beta exceeds the critical beta value at $t = t_c = 3.46$ ms, the resistive SOL modes become unstable. Because of the transport time delay, the divertor sheath temperature, density and the SOL current initially remain at the equilibrium values $t < t_c + \delta t_e = 3.47$ ms. The magnetic perturbation is small and gradually decreases due to the reduction of the pedestal pressure in this initial phase. When the pedestal heat and particles arrive at the divertor sheaths at $t = t_c + \delta t_e$, the the divertor sheath temperature and especially density increase suddenly, and consequently the SOL current surges. The rapid increase of the SOL current gives rise to a rapid increase of the magnetic perturbations in the second phase $t > t_c + \delta t_e$. This positive feedback process defines the bursting feature of ELMs in the numerical results. As the pedestal density and temperature drop to a certain level, the particle and heat sources for the SOL are outbalanced by the cooling and the SOL current reduces. A smaller SOL current leads to a smaller magnetic perturbation. Consequently, an even smaller SOL current results, due to the reduction of the particle and heat sources. This inverted type of positive feedback process leads ELMs to quench sharply. The further heating shown in the first frame of Fig. 1 leads to the next ELM cycle.

It is interesting to discuss the effect of the transport time delay (δt_e and δt_i) under the current ELM physics picture. Note that the connection length of the SOL is about 100 m. The electron transit time from the SOL midplane to divertor is about 2 μs; the ion transit time is about 100 μs, for $T_{e,i} \sim 750$ eV. Because of quasineutrality, the electron transit is decelerated but ion transit is accelerated [17]. In general, the transit time for the discharged electrons depends on the pedestal temperature or collisionality. The larger the pedestal collisionality, the longer the transit time. As shown in Eqs. (7) and (8), a longer transit time results in a larger delay for the response of the divertor sheath temperature and density to the transport from the pedestal. Especially, as discussed earlier, a longer transit time gives rise to a smaller S_n^0, which results in a weaker coupling of the SOL current to the MHD modes. Since the ELM bursting relies on the feedback coupling, a weaker coupling leads to a reduced edge-localizing mode strength. This might explain the experimental observation that the edge-localizing mode strength decreases as the pedestal collisionality increases [2].

In conclusion, we find that the high-n resistive SOL modes can develop into ELMs, if the SOL current is amplified by the modes. The amplification needs a strong heat flux to the SOL; The H mode with high pedestal temperature tends to meet this condition. The proposed model offers a new ELM mechanism that produces a sharp onset and initial fast growth of magnetic perturbation even when the underlying equilibrium is only marginally unstable for an MHD mode and also a quick quenching after the bursting peak. Our picture seems to be consistent with the experimental observation that the ELM bursting occurs at the beta value slightly exceeding the marginal stability limit [18]. Our theory explains also the coexistence of ELMs with the SOL current bursting as observed experimentally [7–9]. We have also discussed the ELM strength dependence on the pedestal collisionality, which is also consistent with the experimental observation [2].

We are grateful to J. W. Van Dam and M. Kotschenreuther for helpful discussion and suggestions. We also acknowledge useful discussion with A. Boozer. Research is supported by Department of Energy Grants No. DE-FG02-04ER54742 and No. DE-AC02-76CH03073.

[1] F. Wagner *et al.*, Phys. Rev. Lett. **49**, 1408 (1982).
[2] A. W. Leonard *et al.*, J. Nucl. Mater. **313–316**, 768 (2003).
[3] P. B. Snyder *et al.*, Phys. Plasmas **12**, 056115 (2005).
[4] H. R. Wilson and S. C. Cowley, Phys. Rev. Lett. **92**, 175006 (2004).
[5] C. G. Gimblett, R. J. Hastie, and P. Helander, Phys. Rev. Lett. **96**, 035006 (2006).
[6] D. A. D'lppolito *et al.*, Contrib. Plasma Phys. **44**, 205 (2004).
[7] H. Takahashi *et al.* , in *Proceedings of the 32nd European Physical Society Conference on Controlled Fusion and Plasma Physics* (Euro. Phys. Soc., Geneva, 2005), p.4.018.
[8] H. Takahashi and E. D. Fredrickson *et al.*, Nucl. Fusion **44**, 1075 (2004).
[9] H. Takahashi, E. D. Fredrickson, and M. J. Schaffer, Phys. Rev. Lett. (to be published).
[10] F. L. Hinton, in *Handbook of Plasma Physics*, edited by M. N. Rosenbluth *et al.* (North-Holland, Amsterdam, 1983) Vol. 1, p. 205.
[11] J. A. Boedo *et al.*, Phys. Plasmas **10**, 1670 (2003).
[12] G. M. Staebler and F. L. Hinton, Nucl. Fusion **29**, 1820 (1989).
[13] A. Boozer, Phys. Plasmas **6**, 3180 (1999).
[14] S. W. Haney and J. P. Freidberg, Phys. Fluids B **1**, 1637 (1989).
[15] R. Fitzpatrick, Phys. Plasmas **14**, 062505 (2007).
[16] B. LaBombard *et al.*, J. Nucl. Mater. **241–243**, 149 (1997).
[17] A. Bergmann, Nucl. Fusion **42**, 1162 (2002).
[18] K. H. Burrell *et al.*, Phys. Plasmas **12**, 056121 (2005).